

Antiferromagnetic Ordering in MnF(salen)

Erik Čížmár,¹ Olivia N. Risset,² Tong Wang,³ Martin Botko,¹ Akhil R. Ahir,² Matthew J. Andrus,² Ju-Hyun Park,⁴ Khalil A. Abboud,² Daniel R. Talham,² Mark W. Meisel,⁵ and Stuart E. Brown³

¹*Department of Condensed Matter Physics, P. J. Šafárik University, Park Angelinum 9, 041 54 Košice, Slovakia*

²*Department of Chemistry, University of Florida, Gainesville, FL 32611-7200, USA*

³*Department of Physics and Astronomy, University of California, Los Angeles, CA 90095-1547, USA*

⁴*National High Magnetic Field Laboratory, Florida State University, Tallahassee, FL 32310-3706, USA*

⁵*Department of Physics and National High Magnetic Field Laboratory, University of Florida, Gainesville, FL 32611-8440, USA*

(Dated: August 10, 2016)

Antiferromagnetic order at $T_N = 23$ K has been identified in Mn(III)F(salen), salen = $\text{H}_{14}\text{C}_{16}\text{N}_2\text{O}_2$, an $S = 2$ linear-chain system. Using single crystals, specific heat studies performed in magnetic fields up to 9 T revealed the presence of a field-independent cusp at the same temperature where ^1H NMR studies conducted at 42 MHz observed dramatic changes in the spin-lattice relaxation time, T_1 , and in the linewidths. Neutron powder diffraction performed on a randomly-oriented, as-grown, deuterated (12 of 14 H replaced by d) sample of 2.2 g at 10 K and 100 K did not resolve the magnetic ordering, while low-field (less than 0.1 T) magnetic susceptibility studies of single crystals and randomly-arranged microcrystalline samples reveal subtle features associated with the transition. Ensemble these data suggest a magnetic signature previously detected at 3.8 T for temperatures below nominally 500 mK is a spin-flop field of small net moments arising from alternating subsets of three Mn spins along the chains.

PACS numbers: 75.50.Ee, 75.40.Cx, 76.60.Es, 75.25.-j

I. INTRODUCTION

After Haldane identified significant differences in the magnetic behavior of integer and half-integer, Heisenberg, antiferromagnetic spins in one-dimension,^{1,2} some time elapsed before $\text{Ni}(\text{C}_2\text{H}_8\text{N}_2)_2\text{NO}_2(\text{ClO}_4)$, commonly referred to as NENP, emerged as a model $S = 1$ system³ that exhibiting no evidence of long-range ordering down to at least 4 mK.^{4,5} With a wide-range of work reported on $S = 1$ Haldane systems,⁶ the challenge of finding an $S = 2$ Haldane system was reportedly resolved with the identification of $\text{MnCl}_3(\text{bpy})$, $\text{bpy} = \text{C}_{10}\text{H}_8\text{N}_2$ (2,2'-bipyridine),^{7,8} as a Haldane gapped system with nearest-neighbor interaction $J \approx 35$ K and no long-range order down to 30 mK.⁹ However, high-field magnetization¹⁰ and EPR studies¹¹ of as-grown microcrystalline samples at low temperature, $T = 1.3$ K, provided evidence of a spin-flop transition and the presence of antiferromagnetic resonance (AFMR) modes. Recently with the use of single crystals, long-range antiferromagnetic ordering has been identified in $\text{MnCl}_3(\text{bpy})$ near 11 K.^{12,13}

Although other candidate $S = 2$ linear-chain materials have been identified,^{6,14–19} these systems possess long-range ordering, and evidence of a gapped quantum spin liquid state just above the ordering was not detected in CrCl_2 .¹⁹ In parallel with these experimental studies, theoretical activity to extend and explore the quantum spin properties of antiferromagnetic $S = 2$ spins in one-dimension is topical and intense.^{20–27}

Recently, a new $S = 2$ linear-chain system, MnF(salen), salen = $\text{H}_{14}\text{C}_{16}\text{N}_2\text{O}_2$, was synthesized, and the low-field, high-temperature magnetic properties were fit with $J/k_B \approx 46$ K, while no evidence of a magnetic

transition was detected down to 1.8 K.²⁸ This report motivated a suite of studies, including torque magnetometry and EPR on single crystals and neutron scattering on a partially deuterated, as-grown, microcrystalline powder-like sample, and a brief report of the resulting data sets are published elsewhere.²⁹ During the course of this work, specific heat and ^1H NMR investigations were initiated, and both experiments provided unambiguous evidence of long-range antiferromagnetic order at $T_N = 23$ K. The purpose of this paper is to present these data sets and the corresponding analyses, which, when combined with neutron powder diffraction at 10 K and 100 K and additional systematic studies of the low-field magnetic response, provide insight into the nature of the magnetic transition.

II. EXPERIMENTAL DETAILS AND RESULTS

A. Material Preparation

All non-deuterated chemical reagents were purchased from Sigma-Aldrich, Alfa Aesar, or Tokyo Chemical Industry (TCI) Company and used without further purification. The deuterated reagents were purchased from C/D/N Isotopes. Using the facilities at the University of Florida, the hydrogenated samples of MnF(salen) were synthesized as described elsewhere.²⁸ The identity and purity of the compound were confirmed by X-ray diffraction and FT-IR spectroscopy. The deuterated sample MnF(salenH2-d12) was prepared following the same procedure²⁸ using deuterated precursors salicylaldehyde-d4 and 2,2-bis(salicylaldehyde)ethylenediimine acid-d12

(salenH2-d12).

Synthesis of salicylaldehyde-d4. Salicylaldehyde-d4 was synthesized using a modification of the method reported elsewhere.³⁰ Paraformaldehyde (110 mmol) was added to phenol-d6 (16 mmol), anhydrous magnesium dichloride (24 mmol) and triethylamine (61 mmol) in 40 mL dry acetonitrile yielding a white suspension. The mixture was refluxed for 8 hours and the resulting yellow suspension was allowed to cool overnight. Water (50 mL) was added and the mixture was acidified with aq. HCl to reach pH = 2. Water was further added to increase the mixture volume to 150 mL. The product was extracted with ether (3×200 mL), dried with magnesium sulfate and evaporated. The resulting orange oil was purified by flash chromatography on silica gel to give a light yellow oil. Yield = 8.9 mmol (56%). ¹H NMR (300 MHz, CDCl₃): 9.83 (s, ¹H, CHO), 10.95 (s, ¹H, OH). FT-IR (cm⁻¹): 3442(broad), 2970(w), 2858(w), 1647(s), 1602(m), 1558(s), 1390(s), 1289(s), 1189(m), 1125(s), 1055(m), 1032(m), 888(m), 857(w), 832(m), 816(m), 751(m), 721(s).

Synthesis of 2,2-bis(salicylaldehyde)ethylenediimine acid-d12 (salenH2-d12). SalenH2-d12 was prepared using a conventional procedure for salen synthesis based on the condensation of salicylaldehyde with ethylenediimine. To a boiling ethanol solution (20 mL) containing salicylaldehyde-d4 (14 mmol), ethylene-d4-diamine (7 mmol) was added dropwise under vigorous stirring. After 10 min, the mixture was cooled in an ice/water bath and the product was filtered, washed with cold ethanol, and air-dried yielding bright yellow flaky crystals. Yield: 5.6 mmol (80%). ¹H NMR (300 MHz, CDCl₃): 8.58 (s, ²H, =CH), 13.37 (s, ²H, OH). FT-IR (cm⁻¹): 3421(broad), 1631(s), 1591(s), 1551(s), 1444(s), 1395(s), 1333(s), 1300(s), 1220(m), 1151(m), 1098(s), 1052(s), 1025(m), 975(m), 857(s), 809(m), 767(m), 737(m), 588(s).

B. Specific heat

The specific heat studies used the facilities located at P. J. Šafárik University and were made with several single crystal samples. In the temperature range between 0.38 K and 40 K, a commercial system (Quantum Design PPMS) equipped with a ³He insert was used while employing the relaxation method technique. Two independent measurements were made, where the first used one single crystal of mass 0.8 mg and the second one employed two crystals of total mass 0.67 mg, and these data are shown in Fig. 1. Below 1 K, the experiment was conducted in a ³He-⁴He dilution refrigerator (Air Liquide Minidil) using a 2.1 mg single crystal. The sample was attached using Apiezon N vacuum grease to the home-made calorimeter consisting of a sapphire substrate, which also supported a thin-layer RuO₂ thermometer and a resistive heater. The RuO₂ thermometer was calibrated against a commercial (Scientific Instruments (SI)) RuO₂-based

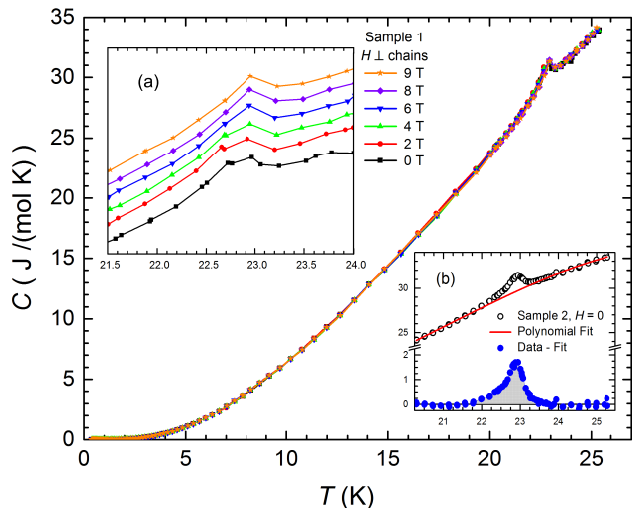


FIG. 1. (Color online) The temperature dependence of the addenda-corrected specific heat measured in magnetic fields ($0 \leq \mu_0 H \leq 9$ T) with H oriented nominally perpendicular to the chains is shown for Sample 1 (0.8 mg). Inset (a) shows an expanded view of the data in the vicinity of the transition, and these data have been vertically shifted for clarity. The solid lines in the main panel and (a) are straight connections between data points. Inset (b) shows the data for Sample 2 (0.67 mg) in zero applied field. A polynomial fit to the data away from the transition region is shown by the solid (red) line. The results of subtracting the fit line from the data are shown at the bottom of the plot. The shaded region provides (*de facto* the area under a C/T curve) an estimate of the entropy change in the vicinity of the transition of 48 mJ/(K mol) or 0.4% of the total magnetic entropy of $R \ln(5) = 13.38$ J/(K mol).

thermometer. The magnetoresistance changes of the SI thermometer were included using a known correction from the literature.³¹ The specific heat was measured down to 60 mK by standard dual-slope and heat-pulse methods,³² which are similar to the ones used in PPMS instrument.

C. NMR

The ¹H NMR studies were performed with standard four-phase cycling Fourier-transform spin-echo techniques using a spectrometer and probe built at UCLA. The sample holder was constructed from teflon and brass, and the coil was wound from teflon-coated wire. The choice of these materials effectively reduced extraneous proton signals to an undetectable level. The circuit was bottom-tuned using fixed matching and tuning elements, and the magnetic field set to the ¹H resonance condition (989.4 mT at 42.130 MHz) using an electromagnet. The sample was cooled in a variable-temperature insert placed in a bucket dewar with its tail between the magnet pole-faces. The sample studied was a single crystal of mass 5.1 mg, with the field aligned orthogonal to the

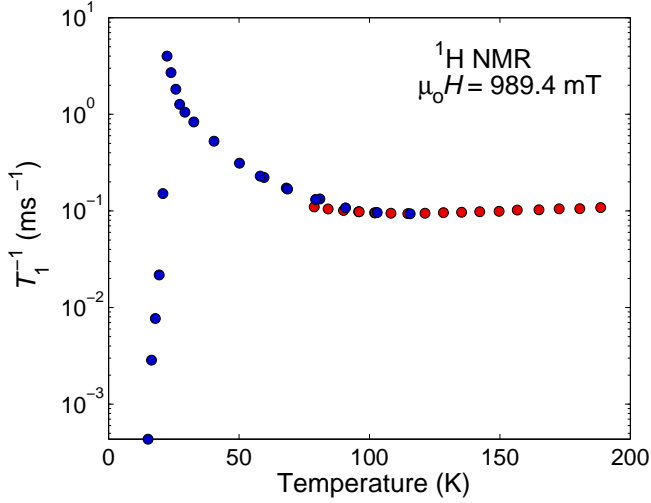


FIG. 2. The temperature dependence of the spin-lattice relaxation rate, T_1^{-1} , in an applied field of 989.4 mT and excitation frequency 42.13 MHz is shown for a single crystal with H nominally aligned along the chain direction when the cryogen employed was helium (blue) or nitrogen (red). The sharp drop below $T_N = 23$ K identifies the antiferromagnetic phase transition.

chain axis.

The temperature dependence of the spin-lattice relaxation rate, T_1^{-1} , is shown in Fig. 2. These data exhibit a relatively weak variation with $T_1^{-1} \sim 100$ s $^{-1}$ down to about 80 K. Further cooling leads to a monotonic increase of almost 2 orders of magnitude before precipitously dropping by many orders of magnitude below $T = 23$ K. The increase over the range 23 K $< T \simeq 80$ K signals the onset of antiferromagnetic correlations and the associated slowing of the fluctuating field. The drop in T_1^{-1} below 23 K is accompanied by a loss of signal intensity associated with the discontinuous onset of line-broadening, most of which is outside the spectrometer operating bandwidth of order 100 kHz. The data were collected while cooling and warming and no hysteresis was detected.

In Fig. 3, two spectra, characteristic of temperatures above and below the ordering temperature, are shown. For $T > T_N$, the linewidth was approximately 50 kHz and exhibited unresolved features that presumably result from inequivalent hyperfine couplings and internuclear spin-spin couplings. For $T < T_N$, the spectrum is much too broad for the pulse conditions ($p_1(\pi/2) = 1.1$ μ s, refocusing pulse $p_2 = 0.7$ μ s). Thus, the full spectrum for the low-temperature phase was constructed from a sum of field-swept spectra recorded at 5 mT intervals. Since the proton gyromagnetic ratio is $\gamma = 42.577$ MHz/T, the equivalent steps in frequency correspond to slightly larger than 200 kHz, and therefore some spectral distortions are certainly present. Nevertheless, in the data, there is a center of symmetry about the unshifted posi-

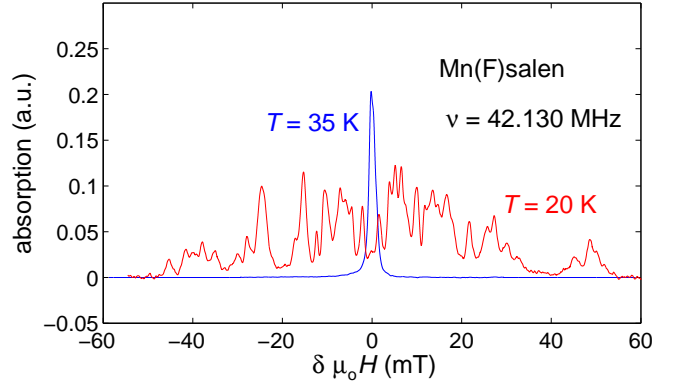


FIG. 3. The two spectra shown are from temperatures greater than (paramagnetic state, narrow line) and less than $T_N = 23$ K. The low temperature spectrum is constructed from a spectral sum, where the echo transients are recorded at 5 mT intervals. $\delta\mu_0 H = 0$ corresponds to an applied field 989.4 mT.

tion. Furthermore, the broadening was observed to onset discontinuously, indicative of a first-order transition, and the overall symmetry of the lineshape is consistent with commensurate magnetic ordering. The overall scale of the broadening (± 2 MHz) is consistent with direct dipolar electron-nuclear spin coupling, when assuming ordered moments of order 1-2 μ_B and a closest ^1H -Mn distance of 3 \AA .

Returning to the nuclear spin-lattice relaxation, a temperature-independent result is expected in the case $k_B T \gg z J$,^{33,34} where the hyperfine-field fluctuations predominantly originate with electronic spin T_2 processes determined by the exchange interaction J and z is the number of nearest neighbors. The relaxation rate in this limit can be estimated as

$$T_{1\infty}^{-1} = \frac{1}{2} \gamma^2 \frac{\hbar^2}{\omega_e} \quad , \quad (1)$$

with ω_e a characteristic frequency for the spectral density, given by $\omega_e^2 = J^2 z S(S+1)/\hbar^2$. To within geometric factors of order unity, the effective mean-square field for electron-nuclear dipolar coupling is

$$h^2 = \frac{[2\pi]^{1/2}}{3} \frac{(\hbar\gamma_e)^2}{\omega_e} S(S+1) \sum_i \langle r_i^{-6} \rangle \quad , \quad (2)$$

where the sum is over the proton-Mn distances for the i^{th} Mn site. If we take the characteristic distance as 4 \AA , the result is $T_{1\infty}^{-1} \sim 10$ s $^{-1}$, which is about an order of magnitude smaller than observed. Presumably the discrepancy arises from a combination of properly estimating the geometric factors, the field orientation, and/or the sum.

D. Neutron Powder Diffraction

Time-of-flight, powder neutron diffraction (TOF-NPD) studies were performed using the POWGEN in-

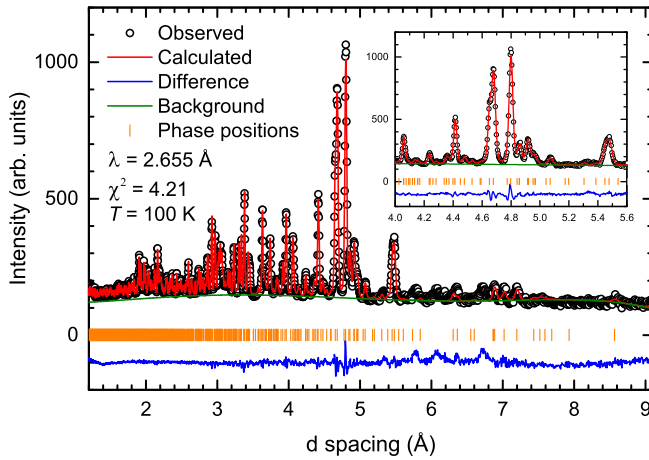


FIG. 4. (Color online) The intensity of the number of counts as a function of the lattice spacing d are shown for the NPD study performed on $\text{MnF}(\text{salenH2-d12})$ at 100 K. The inset shows an expanded view of the results.

strument at Spallation Neutron Source at Oak Ridge National Laboratory. A deuterated $\text{MnF}(\text{salen})$ as-grown, randomly-arranged, powder-like sample with a mass of 2.2 g was placed in a vanadium can that was mounted in an “Orange” cryostat for collecting data at 100 K, shown in Fig. 4, and 10 K. The diffraction patterns were analyzed by Rietveld refinements using General Structure Analysis System package (GSAS) and the graphical user interface (EXPGUI).^{35,36} The data sets collected at both temperatures are essentially equivalent because, over the range of wave-vector measured, it was not possible to refine the 10 K structure with additional magnetic peaks. At 100 K, the unit cell parameters for $\text{MnF}(\text{salenH2-d12})$, Fig. 4, are $a = 10.01714$ Å, $b = 15.43788$ Å, $c = 16.00454$ Å, $\alpha = 108.169^\circ$, $\beta = 103.936^\circ$, and $\gamma = 101.132^\circ$. The detailed analysis of both data sets will be given elsewhere.³⁷

E. Magnetometry

Two commercial magnetometers (Quantum Design MPMS-XL7), one at UCLA and the other at the University of Florida, were used. Previously, several batches, including the deuterated one, of as-grown, randomly arranged microcrystals provided a response similar to the data reported by Birk *et al.*²⁸ Specifically, when using the Padé approximations of quantum Monte Carlo simulations,³⁸ the low-field magnetic susceptibility at high temperatures was well fit when $J = 50 \pm 2$ K for $g = 2$.²⁹ After the discovery of the specific heat and NMR signatures of long-range antiferromagnetic ordering at $T_N = 23$ K, the magnetic susceptibility studies were extended to include a single crystal and zero-field-cooling (ZFC) versus field-cooling (FC) study of a fresh (less than one-month old) as-grown microcrystalline sample. The results shown in Fig. 5 indicate the single crystal sample

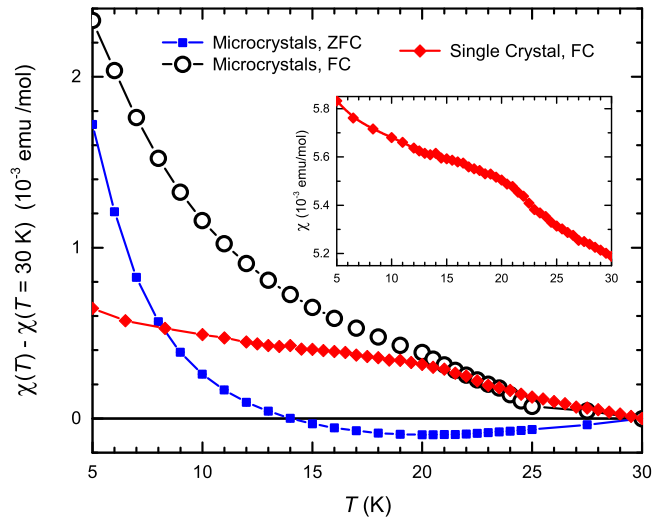


FIG. 5. (Color online) The magnetic susceptibility, referenced to the value measured at 30 K, is shown as a function of temperature. The red diamonds are the data, acquired at 0.1 T with the field nominally along the chains, for the single crystal used in the NMR experiments, and the inset shows the non-normalized values for $5 \text{ K} \leq T \leq 30 \text{ K}$. When zero-field-cooling (ZFC) and field-cooling (FC) studies using 10 mT failed to reveal any detectable differences in the microcrystalline sample as shown by the blue squares, the sample was FC in 7 T from room temperature and subsequently measured while warming in 10 mT as marked by the open circles. All of the lines are guides for the eyes.

possesses a subtle bump near 22 K when a field of 0.1 T is oriented nominally parallel to the chains. Although ZFC and FC studies using 10 mT failed to reveal any variation of the magnetic response for the microcrystalline sample, differences below 30 K were detectable when the FC cycle was repeated in 7 T while cooling from room temperature and subsequently collecting data while warming in 10 mT, Fig. 5.

III. DISCUSSION AND SUMMARY

Firstly, the specific heat data reveal the presence of a small bump at $T_N = 23$ K, and this result is strikingly similar to the results reported for another $S = 2$ quasi-linear chain material $\text{MnCl}_3(\text{bpy})$.¹² In fact, the small value of the magnetic entropy removed at or below the ordering temperature is a signature of the low-dimensionality of the material since the majority of entropy is reduced by the low-dimensional short-range correlations at higher temperature. Other examples of this situation have been reported for the one-dimensional antiferromagnet $(\text{CH}_3)_4\text{NMnCl}_3$, commonly known at TMMC,⁴⁰ for the molecular magnet $[\text{Fe}^{\text{II}}(\Delta)\text{Fe}^{\text{II}}(\Lambda)(\text{ox})_2(\text{Phen})_2]_n$,⁴¹ and the metal-organic framework $\text{Co}_4(\text{OH})_2(\text{C}_{10}\text{H}_{16}\text{O}_4)_3$.⁴² For $\text{MnF}(\text{salen})$, the magnetic contribution can not be separated from the

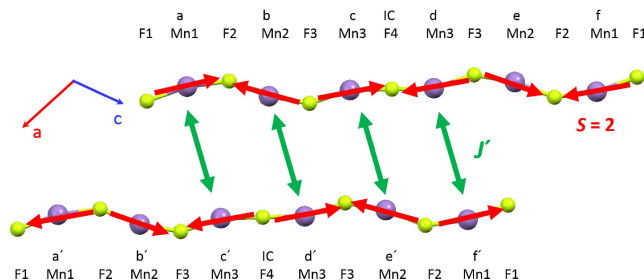


FIG. 6. (Color online) A schematic of the Mn and F atoms of the nearest-neighbor chains is shown, and these chains are not in the same plane as the image. The a-axis and c-axis projections are shown while the b-axis projection is hidden behind the c-axis vector. The labels of the Mn and F atoms follows the notation used by Birk *et al.*^{28,39} The suggested antiferromagnetic arrangement shown by the red arrows is the same possibility described in the Supplemental Information, Fig. SI2, by Birk *et al.*²⁸ The green arrows indicate the conjectured antiferromagnetic interchain coupling J' due to the $H \cdots H$ contacts of < 3 Å between interwoven salen molecules that are not shown. The proposed arrangement indicates a doubling of the lattice unit cell to generate the magnetic unit cell, but the NPD study did not resolve the magnetic structure due to the limited d -spacing that was measured. In addition, a net moment for every subset of three Mn atoms is antiferromagnetically arranged along the chains. The torque magnetometry studies reported by Park *et al.*²⁹ indicate a critical field of 3.8 T for $T \lesssim 500$ mK, and this feature is the spin-flop field of the net moment of each subset of three Mn.

phonon contribution, so an accurate estimate of the total magnetic entropy removed below the ordering temperature is not possible. The only theoretical work, which evaluates the contribution of three-dimensional ordering to the specific heat at the Neél temperature, is reported for the two-dimensional square-lattice including interlayer interaction.⁴³ This theoretical work clearly shows how the entropy removed at the three-dimensional ordering transition is related to the strength of interlayer interaction, where weak-coupling between the planes generates a subtle anomaly in the specific heat as only a tiny portion of entropy is removed. Conjecturing that this type of result might be extended to one-dimensional chains, then one can infer the perturbation preventing the occurrence of a Haldane state for $S = 2$ chains might

be very weak. Additional theoretical consideration of this situation is warranted by the recent findings reported here for MnF(salen) and elsewhere for $MnCl_3(bpy)$.¹²

Secondly, the NMR data from both single crystal and microcrystalline samples indicate a robust, first-order antiferromagnetic transition at $T_N = 23$ K. The increase of T_1^{-1} by almost two orders of magnitude as the temperature is decreased toward T_N is consistent with the slowing of the moments due to increased correlations and the removal of entropy. These results indicate the importance of local probes, such as NMR and muon-spin rotation, that detect the formation of static moments and provide transition signatures commonly missed by standard magnetometry techniques. In addition, the difficulty of thermodynamically observing the transition of MnF(salen) is not caused by the competition between structural coherence and the magnetic correlation length.¹⁷

Finally, all of the results suggest MnF(salen) is antiferromagnetically ordered below 23 K, where the interchain coupling is antiferromagnetic, leading to the conjectured spin arrangement shown in Fig. 6. This arrangement was discussed by Birk *et al.*²⁸ and provides a potential reason why the NPD study of an unorientated microcrystalline sample did not unambiguously detect the magnetic spin arrangement. Of course, an expanded d -spacing NPD study using a single-crystal sample could test this conjecture.

ACKNOWLEDGMENTS

This work was supported, in part, by the National Science Foundation via DMR-1105531 and DMR-1410343 (SEB), DMR-1005581 and DMR-1405439 (DRT), DMR-1202033 (MWM), and DMR-1157490 (NHMFL), by the Slovak Agency for Research and Development APVV-0132-11 and VEGA 0/0145/13 (EC), and by the Fulbright Commission Slovak Republic (MWM). Research at Oak Ridge National Laboratory's Spallation Neutron Source (SNS) was sponsored by the Scientific User Facilities Division, Office of Basic Energy Sciences, U.S. Department of Energy. The NPD experiments were performed by A. Huq, who also provided significant analysis assistance. Discussions with A. Huq, S. E. Nagler, and the coauthors of the earlier studies on this system²⁹ are gratefully acknowledged.

¹ F. Haldane, Physics Letters A **93**, 464 (1983).

² F. D. M. Haldane, Phys. Rev. Lett. **50**, 1153 (1983).

³ J. P. Renard, M. Verdaguer, L. P. Regnault, W. A. C. Erkelens, J. Rossat-Mignod, and W. G. Stirling, EPL (Europhysics Letters) **3**, 945 (1987).

⁴ O. Avenel, J. Xu, J. S. Xia, M.-F. Xu, B. Andraka, T. Lang, P. L. Moyland, W. Ni, P. J. C. Signore, C. M. C. M. van Woerkens, E. D. Adams, G. G. Ihas, M. W. Meisel, S. E. Nagler, N. S. Sullivan, Y. Takano, D. R. Tal-

ham, T. Goto, and N. Fujiwara, Phys. Rev. B **46**, 8655 (1992).

⁵ O. Avenel, J. Xu, J. Xia, M.-F. Xu, B. Andraka, T. Lang, P. Moyland, W. Ni, P. Signore, C. Woerkens, E. Adams, G. Ihas, M. Meisel, S. Nagler, N. Sullivan, Y. Takano, D. Talham, T. Goto, and N. Fujiwara, Journal of Low Temperature Physics **89**, 547 (1992).

⁶ M. Yamashita, T. Ishii, and H. Matsuzaka, Coordination Chemistry Reviews **198**, 347 (2000).

- ⁷ H. A. Goodwin and R. N. Sylva, Australian Journal of Chemistry **20**, 629 (1967).
- ⁸ S. P. Perlepes, A. G. Blackman, J. C. Huffman, and G. Christou, Inorganic Chemistry **30**, 1665 (1991).
- ⁹ G. E. Granroth, M. W. Meisel, M. Chaparala, T. Jolicœur, B. H. Ward, and D. R. Talham, Phys. Rev. Lett. **77**, 1616 (1996).
- ¹⁰ M. Hagiwara, Y. Idutsu, Z. Honda, and S. Yamamoto, Journal of Physics: Conference Series **400**, 032014 (2012).
- ¹¹ M. Hagiwara, M. Ikeda, Y. Idutsu, S. Kimura, and Z. Honda, Journal of the Korean Physical Society **62**, 2046 (2013).
- ¹² M. Hagiwara, S. Shinozaki, A. Okutani, D. Yoshizawa, T. Kida, T. Takeuchi, O. N. Risset, D. R. Talham, and M. W. Meisel, Physics Procedia **in press**, xxx (2015).
- ¹³ S. Shinozaki, A. Okutani, D. Yoshizawa, T. Kida, T. Takeuchi, S. Yamamoto, O. N. Risset, D. R. Talham, M. W. Meisel, and M. Hagiwara, Phys. Rev. B **xx**, zzzzzz (submitted).
- ¹⁴ G. E. Granroth, Ph.D. thesis, University of Florida (1998), <https://archive.org/details/experimentalstud00gran>.
- ¹⁵ Y. Matsushita and Y. Ueda, Inorganic Chemistry **42**, 7830 (2003).
- ¹⁶ P. Lone, G. Andr, C. Doussier, and Y. Molo, Journal of Magnetism and Magnetic Materials **284**, 92 (2004).
- ¹⁷ E. Čizmar, J.-H. Park, S. Gamble, B. Ward, D. Talham, J. Tol, L.-C. Brunel, M. Orendáč, A. Feher, J. Šebek, and M. W. Meisel, Journal of Magnetism and Magnetic Materials **272-276, Part 2**, 874 (2004), proceedings of the International Conference on Magnetism (ICM 2003).
- ¹⁸ C. Stock, L. C. Chapon, O. Adamopoulos, A. Lappas, M. Giot, J. W. Taylor, M. A. Green, C. M. Brown, and P. G. Radaelli, Phys. Rev. Lett. **103**, 077202 (2009).
- ¹⁹ M. B. Stone, G. Ehlers, and G. E. Granroth, Phys. Rev. B **88**, 104413 (2013).
- ²⁰ S. C. Furuya, M. Oshikawa, and I. Affleck, Phys. Rev. B **83**, 224417 (2011).
- ²¹ T. Tonegawa, K. Okamoto, H. Nakano, T. Sakai, K. Nomura, and M. Kaburagi, Journal of the Physical Society of Japan **80**, 043001 (2011).
- ²² H.-H. Tu and R. Orús, Phys. Rev. B **84**, 140407 (2011).
- ²³ F. Pollmann, E. Berg, A. M. Turner, and M. Oshikawa, Phys. Rev. B **85**, 075125 (2012).
- ²⁴ Y.-C. Tzeng, Phys. Rev. B **86**, 024403 (2012).
- ²⁵ K. Hasebe and K. Totsuka, Phys. Rev. B **87**, 045115 (2013).
- ²⁶ J. A. Kjäll, M. P. Zaletel, R. S. K. Mong, J. H. Bardarson, and F. Pollmann, Phys. Rev. B **87**, 235106 (2013).
- ²⁷ A. Kshetrimayum, H.-H. Tu, and R. Orús, Phys. Rev. B **91**, 205118 (2015).
- ²⁸ T. Birk, K. S. Pedersen, S. Piligkos, C. A. Thuesen, H. Weihe, and J. Bendix, Inorganic Chemistry **50**, 5312 (2011).
- ²⁹ J.-H. Park, O. N. Risset, M. Shiddiq, M. K. Peprah, E. S. Knowles, M. J. Andrus, C. C. Beedle, G. Ehlers, A. Podlesnyak, E. Cizmar, S. E. Nagler, S. Hill, D. R. Talham, and M. W. Meisel, Acta Physica Polonica A **126**, 228 (2014).
- ³⁰ N. U. Hofsløkken and L. Skattebøl, Acta Chemica Scandinavica **53**, 258 (1999).
- ³¹ M. Watanabe, M. Morishita, and Y. Ootuka, Cryogenics **41**, 143 (2001).
- ³² J. S. Hwang, K. J. Lin, and C. Tien, Review of Scientific Instruments **68**, 94 (1997).
- ³³ T. Moriya, Progress of Theoretical Physics **16**, 23 (1956).
- ³⁴ T. Moriya, Progress of Theoretical Physics **16**, 641 (1956).
- ³⁵ A. C. Larson and R. B. V. Dreele, Los Alamos National Laboratory Report LAUR **86-748** (2004).
- ³⁶ B. H. Toby, Journal of Applied Crystallography **34**, 210 (2001).
- ³⁷ A. R. Ahir, Ph.D. thesis, University of Florida (anticipated in 2016).
- ³⁸ J. M. Law, H. Benner, and R. K. Kremer, Journal of Physics: Condensed Matter **25**, 065601 (2013).
- ³⁹ Note the correction of a couple of typos in Birk *et al.*, Ref. 27, where the labels Mn1 and Mn3 were switched in their Fig. 1, while the angles Mn1-F2-Mn2 and Mn2-F3-Mn3 were incorrectly given in the text and should be 150.43° and 151.72°, respectively.
- ⁴⁰ F. Borsa, M. G. Pini, A. Rettori, and V. Tognetti, Phys. Rev. B **28**, 5173 (1983).
- ⁴¹ C. J. Ho, J. L. Her, C. P. Sun, C. C. Yang, C. L. Huang, C. C. Chou, L.-L. Li, K. J. Lin, W. H. Li, J. W. Lynn, and H. D. Yang, Phys. Rev. B **76**, 224417 (2007).
- ⁴² R. Sibille, T. Mazet, B. Malaman, T. Gaudisson, and M. Franois, Inorganic Chemistry **51**, 2885 (2012).
- ⁴³ P. Sengupta, A. W. Sandvik, and R. R. P. Singh, Phys. Rev. B **68**, 094423 (2003).